SUPPLEMENTARY MATERIALS: A PROBABILISTIC NUMERICAL EXTENSION OF THE CONJUGATE GRADIENT METHOD*

TIM W. REID†, ILSE C. F. IPSEN†, JON COCKAYNE‡, AND CHRIS J. OATES§

SM1. Supplemental Numerical Experiments. We perform additional numerical experiments to show the behavior of the S-statistic and BayesCG in different situations. The numerical experiments are:

- (Section SM1.1) The same experiments as section 5 but switching the version of the Gauss-Radau estimate used with each matrix
- (Section SM1.2) An examination of the effect reorthogonalization has on the S-statistic
- (Section SM1.3) A comparison the convergence of BayesCG with different choices of prior covariance
- (Section SM1.4) The same experiment as section 5.3 but without preconditioning

These experiments largely have the same setup as in section 5. We explain the differences for each experiment in their respective section.

As in section 5.1, we refer to the Gauss-Radau estimates as

(a) Upper bound [SM9, Section 4]. This is an upper bound of the $\mathbf{A}$-norm error $\|\mathbf{x}_* - \mathbf{x}_m\|_{\mathbf{A}}^2$, it is computed with CGQ, and it requires a lower bound of the smallest eigenvalue of $\mathbf{A}$.

(b) Approximation [SM10, Sections 6 and 8.2]. This is an approximation of the Gauss-Radau upper bound (a). It does not require an eigenvalue bound because it approximates the smallest Ritz value instead.

SM1.1. Switching the Gauss-Radau Estimates. We rerun the experiments from section 5 except the Gauss-Radau approximation (b) is computed for the $n = 48$ matrix and the Gauss-Radau bound (a) is computed for the $n = 11948$ matrix. We use $9 \cdot 10^{-14}$ as the eigenvalue bound needed for the Gauss-Radau bound (a). We chose this bound by computing the smallest eigenvalue, which is $9.0499 \cdot 10^{-14}$, with the inverse power method.

The results are plotted in Figures SM1.1 and SM1.2, which should be compared to Figures 5.2 and 5.4 respectively.

The Gauss-Radau approximation (b) in Figure SM1.1 behaves similarly to the one-sided credible interval $[\mu, S_{95}]$ from (5.1). It underestimates the error when convergence is slow, the first 90 iterations, and it overestimates the error when convergence is fast, from iteration 90 to 120. The right plot of Figure SM1.1 shows that the Gauss-Radau approximation (b) is further from the error than credible interval bound S_{95}. The Gauss-Radau approximation (b) in Figure SM1.1 is further from the error than the Gauss-Radau bound (a) in Figure 5.2, except for the first few iterations.

*Submitted to the editors

Funding: The work was supported in part by NSF grant DMS-1745654 (TWR, ICFI), NSF grant DMS-1760374 (ICFI), and the Lloyd's Register Foundation Programme on Data Centric Engineering at the Alan Turing Institute (CJO).

†Department of Mathematics, North Carolina State University, Raleigh, NC 27695-8205, USA, (twreid@ncsu.edu, ipsen@ncsu.edu)

‡The Alan Turing Institute, 96 Euston Road, London NW1 2DB, UK (jcockayne@turing.ac.uk)

§School of Mathematics, Statistics and Physics, Newcastle University, Newcastle upon Tyne NE1 7RU, UK (chris.oates@ncl.ac.uk)

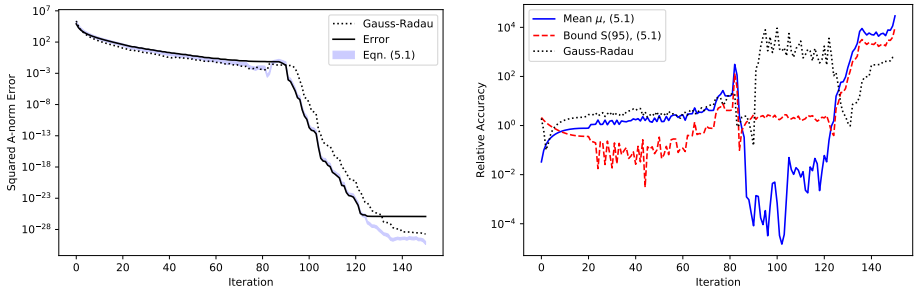

Figure SM1.1: Same as Figure 5.2 except with the Gauss-Radau approximation (b) instead of the bound (a). On the left: upper credible interval $[\mu, S_{95}]$ from (5.1), and Gauss-Radau approximation (b). On the right: relative accuracy ρ from (5.4) for the mean μ and bound S_{95} from (5.1) as well as the Gauss-Radau approximation (b).

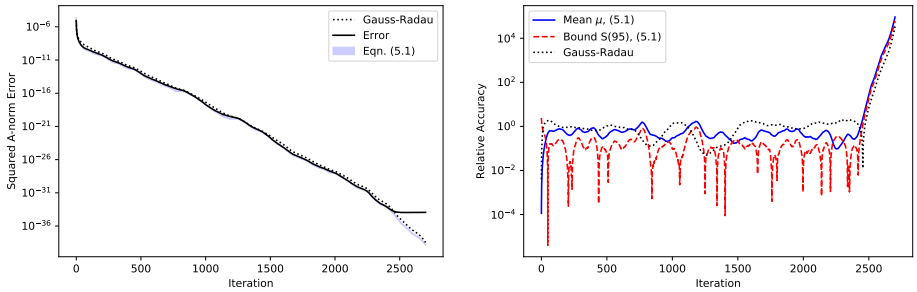

Figure SM1.2: Same as Figure 5.4 except with the Gauss-Radau bound (a) instead of the approximation (b). On the left: upper credible interval $[\mu, S_{95}]$ from (5.1), and Gauss-Radau bound (a). On the right: relative accuracy ρ from (5.4) for the mean μ and bound S_{95} from (5.1) as well as the Gauss-Radau bound (a).

The Gauss-Radau bound (a) in Figure SM1.2 overestimates the error until maximal attainable accuracy is reached, and its relative accuracy (5.4) is comparable to the S-statistic mean. The Gauss-Radau bound (a) in Figure SM1.2 is closer to the error than the Gauss-Radau approximation (b) in Figure 5.4.

This experiment reinforces the conclusion of section 5: the S_{95} credible interval bound is competitive with the Gauss-Radau error estimates. Additionally, this experiment shows that the Gauss-Radau bound (a) performs better than the Gauss-Radau approximation (b) provided an accurate lower bound to eigenvalues of $\mathbf{A}$ are available.

SM1.2. Effect of Reorthogonalization. The exact arithmetic performance of CG is simulated in [SM6, Section 2] by reorthogonalizing the residual vectors. We similarly reorthogonalize Algorithm 3.1 to examine the effect finite precision arithmetic has on the S-statistic.

Setup. This numerical experiment is similar to section 5.2 but with a larger matrix. The matrix is a $n = 500$ random matrix $\mathbf{A} = \mathbf{Q}\mathbf{D}\mathbf{Q}^T$, where $\mathbf{Q}$ is a random

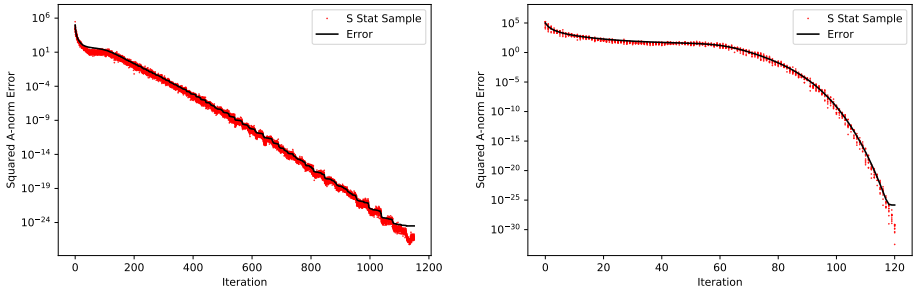

(i.) S-statistic samples s_i from (5.2).

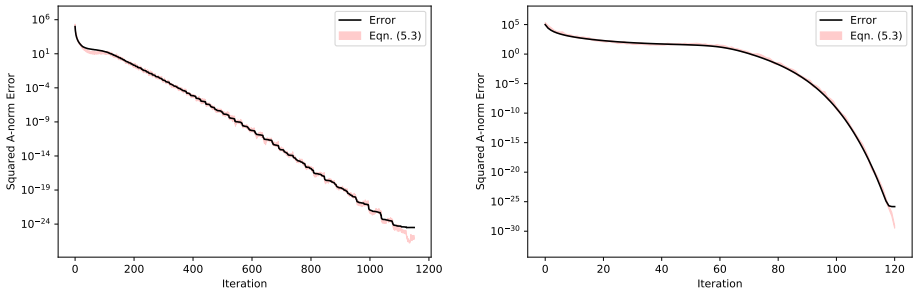

(ii.) Empirical S-statistic credible interval (5.3).

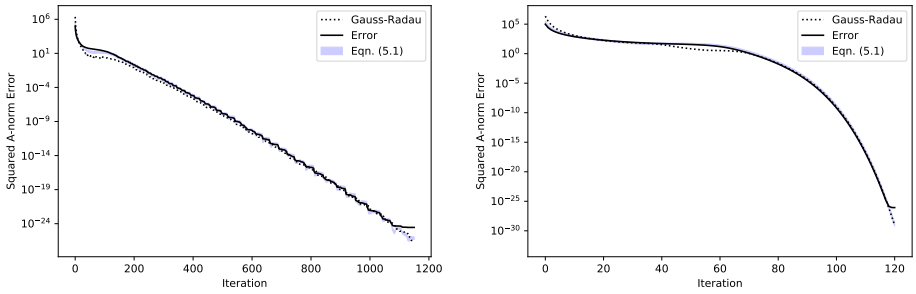

(iii.) One-sided credible interval $[\mu, S_{95}]$ (5.1) and Gauss-Radau approximation (b).

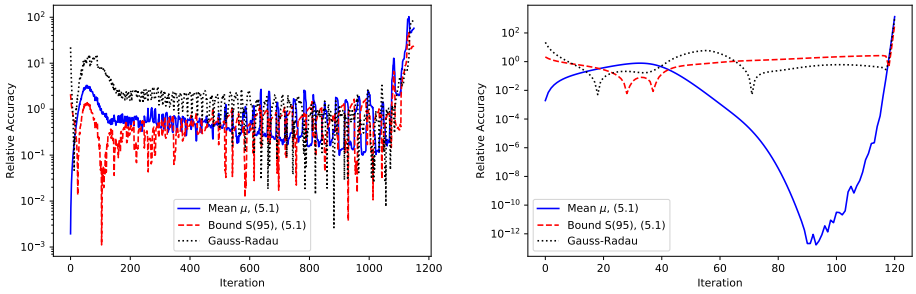

(iv.) Relative accuracy ρ from (5.4) of mean μ (5.1), credible interval bound S_{95} (5.1), and Gauss-Radau approximation (b).

Figure SM1.3: Effect of reorthogonalization on convergence of Algorithm 3.1 and error estimates. On the left: no reorthogonalization. On the right: reorthogonalization.

orthogonal matrix and $\mathbf{D}$ is a diagonal matrix with eigenvalues

$$d_{ii} = 0.1 + \frac{i-1}{n-1}\left(10^4 - 0.1\right)(0.9)^{n-i}, \qquad 1 \leq i \leq 500.$$

This is the eigenvalue distribution that causes roundoff errors in CG [SM12, Section 2], and is the same distribution as in section 5.2.

We compute the upper one-side credible interval $[\mu, S_{95}]$ (5.1) and the Gauss-Radau approximation (b) with the posterior covariance rank (delay) $d = 20$.

Description of Reorthogonalization. The choice to reorthogonalize the residuals in CG—and therefore Algorithm 3.1—relies on two observations: (I) reorthogonalizing the basis vectors in the Lanczos method mitigates the effects of rounding errors [SM11, Section 6], and (II) the residuals in CG are proportional to the Lanczos basis vectors [SM9, Section 2.1]. We implement reorthogonalization in Algorithm 3.1 with Classical Gram-Schmidt performed twice because it can be implemented efficiently and produces vectors that are orthogonal close to machine precision [SM3, SM4].

Results. Convergence of the A-norm error, S-statistic and Gauss-Radau approximation (b), and relative accuracy of the error estimates with and without reorthogonalization are plotted in Figure SM1.3. Reorthogonalization causes the posterior mean $\mathbf{x}_m$ to converge to $\mathbf{x}_*$ much faster.

Fast convergence causes the mean μ from (5.1), which is equal to the error underestimate in [SM13, (4.9)], to be more accurate [SM13, Section 4]. This is because (4.1) implies

$$\|\mathbf{x}_* - \mathbf{x}_m\|_{\mathbf{A}}^2 - \mu = \|\mathbf{x}_* - \mathbf{x}_{m+d}\|_{\mathbf{A}}^2, \tag{SM1.1}$$

and $\|\mathbf{x}_* - \mathbf{x}_{m+d}\|_{\mathbf{A}}^2$ is smaller when convergence is fast.

Reorthogonalization increases convergence speed because it mitigates the effects of the accumulated round off errors which slow CG. A detailed treatment of delay of convergence in CG can be found in [SM8, Section 5.9.1]. CG is usually not reorthogonalized because its computational cost exceeds its benefits.

Reorthogonalization does not have as large an effect on the credible interval bound S_{95} from (5.1) or Gauss-Radau approximation (b), however in section SM1.4 we discuss how slow convergence can negatively affect these estimates.

SM1.3. BayesCG Convergence with Different Priors. We compare the convergence of BayesCG posterior mean with different choices of prior covariance on two $n = 48$ linear systems. The prior covariances we examine are

- Krylov prior, $\mathbf{\Sigma}_0 = \mathbf{\Gamma}_0$
- Inverse prior, $\mathbf{\Sigma}_0 = \mathbf{A}^{-1}$
- Identity prior, $\mathbf{\Sigma}_0 = \mathbf{I}$
- Error prior, $\mathbf{\Sigma}_0 = (\mathbf{x}_* - \mathbf{x}_0)(\mathbf{x}_* - \mathbf{x}_0)^T$

The prior mean for all choices of covariance is the zero vector, $\mathbf{x}_0 = \mathbf{0}$.

Setup. As in section 5, both linear systems are defined by a random matrix, $\mathbf{A} = \mathbf{Q}\mathbf{D}\mathbf{Q}^T$, and the solution vector of all ones, $\mathbf{x}_* = \mathbf{1}$. The two linear systems differ in their eigenvalue distribution $\mathbf{D}$. The first eigenvalue distribution is (5.5), the distribution that causes round off errors in CG [SM12, Section 2]. The second is the geometric eigenvalue distribution [SM5, Section 3.1]:

$$d_{ii} = (10^5)^{(i-1)/(n-1)}. \tag{SM1.2}$$

The condition number resulting from both distributions is 10^5.

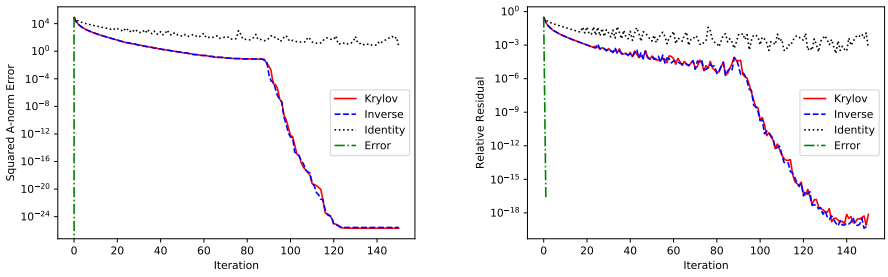

(i.) Same $n = 48$ matrix as in section 5.2

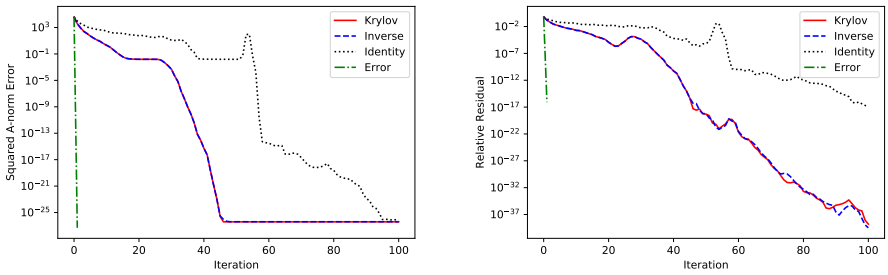

(ii.) $n = 48$ matrix with random eigenvalue distribution (SM1.2)

Figure SM1.4: Convergence of posterior mean $\mathbf{x}_m$ in BayesCG with different choices of prior covariance. On the left: absolute $\mathbf{A}$-norm error $\|\mathbf{x}_* - \mathbf{x}_m\|_{\mathbf{A}}^2$. On the right: relative residual $\frac{\|\mathbf{r}_m\|_2}{\|\mathbf{A}\|_2\|\mathbf{x}_*\|_2}$.

The the posterior mean is computed with Algorithm 3.1 for the Krylov prior and Algorithm 2.1 without reorthogonalization for the inverse, identity, and error priors. The inverse prior is computed as $\mathbf{\Sigma}_m = \mathbf{A}^{-1} = \mathbf{Q}\mathbf{D}^{-1}\mathbf{Q}^T$.

Results. The convergence of the posterior mean resulting from the four priors is plotted in Figure SM1.4. The results are similar for both matrices $\mathbf{A}$. The error prior causes BayesCG to converge in one iteration, the identity prior causes slow convergence, the inverse prior causes relatively fast convergence, and the Krylov prior causes BayesCG to converge at nearly the same speed as the Krylov prior.

These results indicate BayesCG performs as expected. Example 2.11 shows that the error prior should cause BayesCG to converge in one iteration. Convergence with the identity prior is expected to be slow because the BayesCG mean vectors are equal to preconditioned CG iterates with $\mathbf{\Sigma}_0\mathbf{A}$ as the preconditioner [SM7]. Convergence with the Krylov and inverse priors should be the same because Algorithm 3.1 implements BayesCG under Krylov prior as CG and [SM2] shows that the inverse prior causes the mean vector iterates to be equal to CG iterates. The small difference in convergence with the Krylov and inverse priors is likely due to additional round off errors in the three matrix vector products required by Algorithm 2.1.

SM1.4. Large Matrix Without Preconditioning. We repeat the experiment in section 5.3 except without a preconditioner, meaning $\mathbf{A}$ is `bcsstk18` from

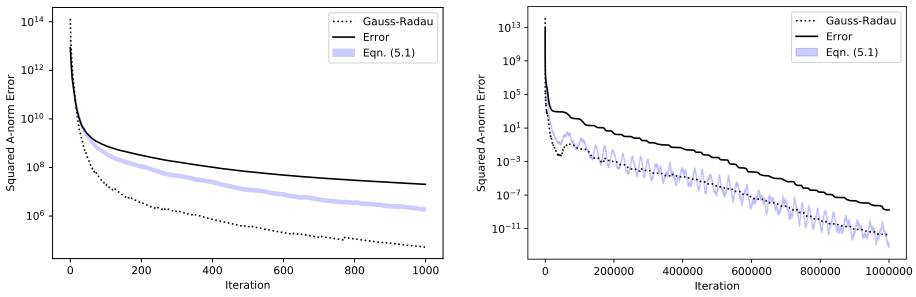

Figure SM1.5: Same as left plot of Figure 5.4. Squared $\mathbf{A}$-norm error $\|\mathbf{x}_* - \mathbf{x}_m\|_{\mathbf{A}}^2$, one-sided credible interval $[\mu, S_{95}]$ from (5.1), and Gauss-Radau approximation (b) versus iterations m. On the left: First 1000 iterations. On the right: 1 Million iterations.

the Harwell-Boeing collection [SM1]. We plot the results in Figure SM1.5. We do not compute any S-statistic samples because of the large amount of iterations required for the error to converge.

It takes over 1 million iterations for the error to reach the maximal attainable accuracy without a preconditioner. This is significantly more than in Figure 5.4 when only the 2500 iterations were required. The one-sided credible interval $[\mu, S_{95}]$ (5.1) as well as the Gauss-Radau approximation (b) underestimate the error by at least an order of magnitude, which is worse than the performance in Figure 5.4.

The speed of convergence impacts the effectiveness of the S-statistic as an error estimate. The credible interval $[\mu, S_{95}]$ (5.1) depends on the mean μ, and the distance between μ and the error (SM1.1) depends on convergence speed. As a consequence, the mean and credible interval are far from the error when convergence is slow.

Convergence speed can also affect the Gauss-Radau approximation (b). The convergence rate of the smallest Ritz value to the smallest eigenvalue is usually related to convergence of the $\mathbf{A}$-norm error [SM10, Section 8.1 and Figures 3 and 4]. Slow convergence of the $\mathbf{A}$-norm means the Ritz value has not converged to the smallest eigenvalue, and this causes the Gauss-Radau approximation (b) to be less accurate.

REFERENCES

[SM1] *BCSSTK18: BCS Structural Engineering Matrices (linear equations) R.E. Ginna Nuclear Power Station*, https://math.nist.gov/MatrixMarket/data/Harwell-Boeing/bcsstruc2/bcsstk18.html.

[SM2] J. Cockayne, C. J. Oates, I. C. F. Ipsen, and M. Girolami, *A Bayesian conjugate gradient method (with discussion)*, Bayesian Anal., 14 (2019), pp. 937–1012, https://doi.org/10.1214/19-BA1145. Includes 6 discussions and a rejoinder from the authors.

[SM3] L. Giraud, J. Langou, M. Rozložník, and J. van den Eshof, *Rounding error analysis of the classical Gram-Schmidt orthogonalization process*, Numer. Math., 101 (2005), pp. 87–100, https://doi.org/10.1007/s00211-005-0615-4.

[SM4] L. Giraud, J. Langou, and M. Rozloznik, *The loss of orthogonality in the Gram-Schmidt orthogonalization process*, Comput. Math. Appl., 50 (2005), pp. 1069–1075, https://doi.org/10.1016/j.camwa.2005.08.009.

[SM5] A. Greenbaum, *Estimating the attainable accuracy of recursively computed residual methods*, SIAM J. Matrix Anal. Appl., 18 (1997), pp. 535–551, https://doi.org/10.1137/S0895479895284944.

[SM6] A. Greenbaum and Z. Strakoš, *Predicting the behavior of finite precision Lanczos and*

conjugate gradient computations, SIAM J. Matrix Anal. Appl., 13 (1992), pp. 121–137, https://doi.org/10.1137/0613011.

[SM7] L. Li and E. X. Fang, *Invited discussion for A Bayesian conjugate gradient method*, Bayesian Anal., 14 (2019), pp. 937–1012, https://doi.org/10.1214/19-BA1145.

[SM8] J. Liesen and Z. Strakos, *Krylov Subspace Methods: Principles and Analysis*, Oxford University Press, 2013.

[SM9] G. Meurant and P. Tichý, *On computing quadrature-based bounds for the A-norm of the error in conjugate gradients*, Numer. Algorithms, 62 (2013), pp. 163–191, https://doi.org/10.1007/s11075-012-9591-9.

[SM10] G. Meurant and P. Tichý, *Approximating the extreme Ritz values and upper bounds for the A-norm of the error in CG*, Numer. Algorithms, 82 (2019), pp. 937–968, https://doi.org/10.1007/s11075-018-0634-8.

[SM11] C. C. Paige, *The Computation of Eigenvalues and Eigenvalues of Very Large Sparse Matrices*, PhD thesis, University of London, 1971.

[SM12] Z. Strakoš, *On the real convergence rate of the conjugate gradient method*, Linear Algebra Appl., 154/156 (1991), pp. 535–549, https://doi.org/10.1016/0024-3795(91)90393-B.

[SM13] Z. Strakoš and P. Tichý, *On error estimation in the conjugate gradient method and why it works in finite precision computations*, Electron. Trans. Numer. Anal., 13 (2002), pp. 56–80.